# Graphene gas pumps

Davidovikj, Dejan; Bouwmeester, Damian; Van Der Zant, Herre S.J.; Steeneken, Peter G.

**DOI**
10.1109/MEMSYS.2018.8346632

**Publication date**
2018

**Document Version**
Final published version

**Published in**
Proceedings 2018 IEEE Micro Electro Mechanical Systems (MEMS 2018)

# GRAPHENE GAS PUMPS

*Dejan Davidovikj[1], Damian Bouwmeester[1], Herre S. J. van der Zant[1], and Peter G. Steeneken[1,2]*
[1]Kavli Institute of Nanoscience, Delft University of Technology,
Delft, THE NETHERLANDS
[2]Department of Precision and Microsystems Engineering, Delft University of Technology,
Delft, THE NETHERLANDS

## ABSTRACT

We report on a pneumatically coupled graphene pump system, comprising two cylindrical cavities of 3 femtoliter connected by a narrow trench, all covered by a thin few-layer graphene membrane. Local electrodes at the bottom of each cavity enable electrostatic pressure control and manipulation of gas flow through the channel. Using laser interferometry, we measure graphene displacement as a function of driving amplitude and frequency, thus providing proof-of-principle for using graphene membranes to pump attoliter quantities of gases and demonstrating pneumatic actuation at the nanoscale.

## INTRODUCTION

Pumps have been of importance for humanity since early civilization. The Egyptians used a contraption called "shadoof" to be able to take out water from the Nile that was used for irrigation. As technology progressed, better pumps and pneumatic systems using higher pressure, larger flow, and hence, higher power have been developed. During the last decades microscale pumps have been receiving great interest for precise control, dosing and mixing of fluids and gases in biological, medical and consumer electronics applications. Moreover, pumps are of interest for driving pneumatic actuators in MEMS and NEMS motors. With respect to the first electrostatically actuated membrane pumps [1, 2], that were presented more than 25 years ago, a tremendous reduction in size has been achieved. Downscaling of dimensions can enable smaller and more precise devices for controlling fluids and gases at the nanoscale [3–5]. The properties of graphene, like its atomic scale thickness and extreme flexibility, are very promising for further miniaturization of nanofluidic devices.

Since the first realization of mechanical graphene devices [6], suspended 2D materials have attracted increasing attention in the MEMS/NEMS community. Many device concepts have been proposed, including pressure sensors [7, 8], gas sensors [9, 10], mass sensors [11, 12], and graphene microphones [13, 14]. The high tension and low mass of graphene membranes have also inspired their implementation as high-speed microactuators in microloudspeakers [15]. Another attractive aspect of graphene membranes is their hermeticity [16] and the ability to controllably introduce pores that are selectively permeable to gases [9].

Although gas damping forces limit graphene's Q-factor at high frequencies, they provide a useful but little explored route towards graphene pumps and nanofluidics. For efficient pumps and pneumatics it is essential that most of the available force is used to move and pressurize the fluid, while minimizing the force required to accelerate and flex the pump membrane. In these respects, the low mass and high flexibility, combined with the impermeability of graphene membranes [16] provide clear advantages.

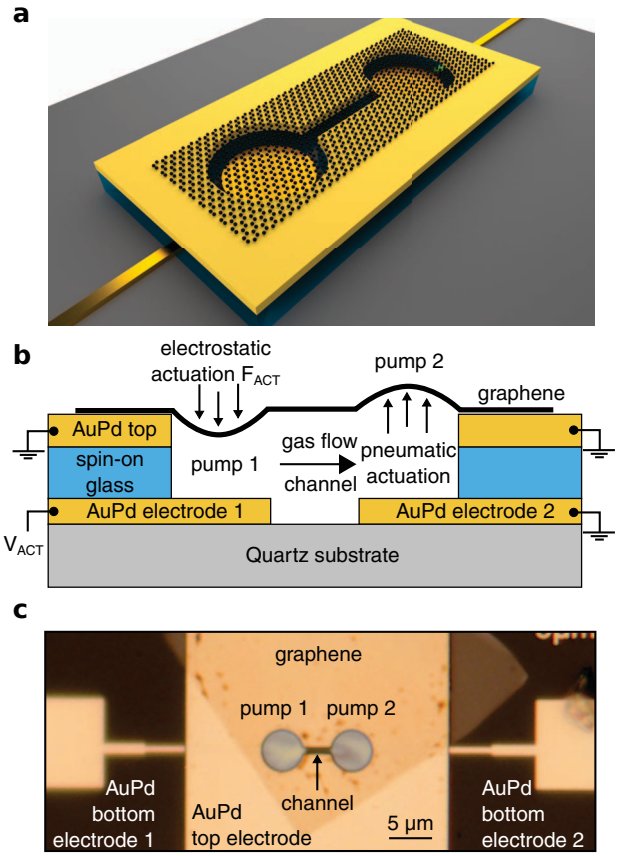


*Figure 1: (a) A 3D schematic of the device: the graphene flake is covering two circular cavities that are connected through a narrow trench. (b) Schematic cross-section of the pumps and actuation mechanism for the case that pump 1 is actuated. (c) Optical micrograph of the device.*

Here, we fabricate a system of two nanochambers ($V_{total}$≈7 fl) coupled by a narrow trench and sealed using a few-layer graphene flake. By designing a chip with individually accessible electrodes we construct a graphene micropump, capable of manipulating the gas flow between the two chambers using small driving voltages ($V_{ACT}$≤1 V). Increasing the gas pressure in one of the nanochambers results in pneumatic actuation of the graphene drum that covers the other nanochamber via the connecting gas channel. To measure the displacement of the drums, we use laser interferometry and demonstrate successful pumping of gas using two pneumatically coupled graphene nanodrums.

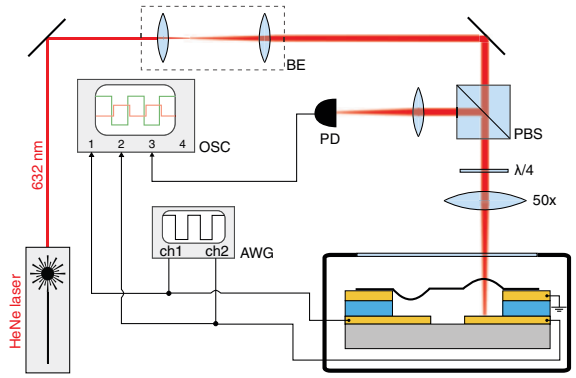


*Figure 2: Setup for electrostatic actuation and interferometric motion readout of either of the pumps. PD: photodiode, OSC: oscilloscope, AWG: arbitrary waveform generator, BE: beam expander and PBS: polarized beam splitter.*

## EXPERIMENT

The device concept is presented in Figure 1a. Two circular AuPd electrodes at the cavity bottom (one for addressing each of the membranes) are separated by a thin layer (130 nm) of spin-on-glass (SOG) silicon oxide from the top metallic (AuPd) electrode. The few-layer (FL) graphene flake (black), with a thickness of 9 monolayers (4 nm), is in direct electrical contact with this top electrode. The entire device is fabricated on top of a quartz substrate to minimize capacitive cross-talk. The device fabrication is described in detail in [17]. A cross-section along the direction of the trench of the device is shown in Figure 1b, which illustrates the working principle. The actuation voltage $V_{ACT,1}$ is applied between AuPd electrode 1 and ground, while keeping AuPd electrode 2 and the AuPd top electrode grounded. As a result, pump 1 experiences an electrostatic force $F_{ACT}$, causing it to deflect downwards. This compresses the gas underneath the membrane and the induced pressure difference causes a gas flow through the channel between the two nanochambers. This results in a pressure increase that causes the other membrane (pump 2) to bulge upwards. Figure 1c shows an optical image of the measured device. The image shows the two bottom electrodes, together with the top metallic island on which the dumbbell shape is patterned. Graphene is transferred last (using an all-dry transfer technique [18]) and it is visible in the image as a darker area on top of the metallic island.

## READOUT

The readout of the motion of the drums is performed using a laser interferometer, shown schematically in Figure 2. A red HeNe laser is focused on one of the graphene membranes, and the sample is mounted in a pressure chamber in a $N_2$ environment at ambient pressure and room temperature. When the membrane moves, the optical interference between the light reflected from the bottom electrode and the light reflected from the graphene causes the light intensity on the photodiode detector to depend strongly on the drum position. By lateral movement of the laser spot, the motion of either of the pumps can be detected. The photodiode signal is read out via an internal first-order low-pass filter with a cut-off frequency of 50 kHz.

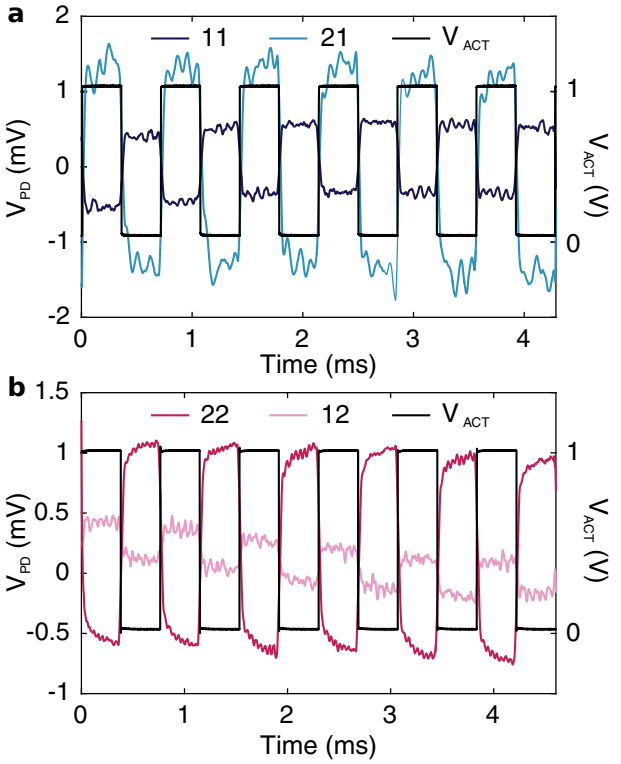


*Figure 3: (a) Measured displacement (photodiode voltage) of drum 1 when actuating drum 1 (measurement 11) and drum 2 (measurement 21). (b) Measured displacement (photodiode voltage) of drum 2 when actuating drum 1 (measurement 12) and drum 2 (measurement 22). The actuation voltage is shown on the right y-axis. Measurements of each of the drums are performed at constant laser position to ensure that the transduction of the system ($V_{PD}/z$) is constant.*

For electrostatic actuation, the two bottom electrodes are connected to two channels of an arbitrary waveform generator, where one is grounded and the other one is actuated (Figs. 1b and 2). The actuation voltage ($V_{ACT}$) on each of the drums and the photodiode voltage ($V_{PD}$) are measured using an oscilloscope. The top electrode (i.e. the graphene flake) is electrically grounded during the measurements. Since there are 2 pumps that can be actuated (pump 1 and pump 2) and either of them can be detected with the red laser there are 4 measurement configurations indicated by $V_{PD,11}$, $V_{PD,21}$, $V_{PD,12}$ and $V_{PD,22}$, where the first number indicates the pump that is actuated and the second number indicates the pump that is read out by the laser.

## GAS PUMP & PNEUMATIC ACTUATION

Pneumatic actuation is one of the most efficient ways to transfer force over large distances in small volumes. At the microscale, the pneumatic coupling also has the advantage of converting the attractive downward electrostatic force on pump 1 to an upward force on the graphene membrane of pump 2 (Fig 1b). Thus, proof for gas pumping and pneumatic actuation can be obtained by detecting that the motion of both drums is in opposite directions.

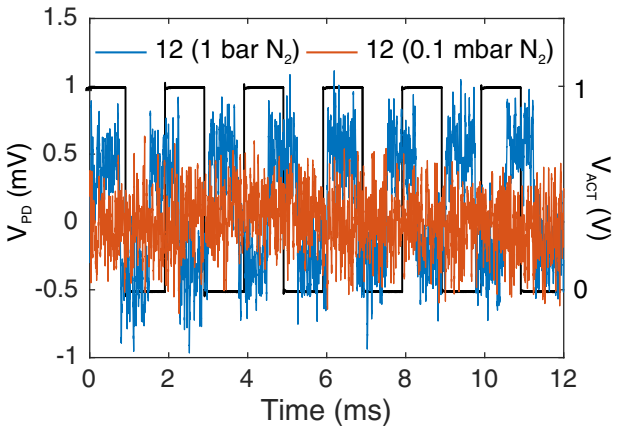


*Figure 4: Measurement of the motion of pump 2 when actuating pump 1 at atmospheric pressure (blue curve) and in vacuum (orange curve).*

The drums are actuated using a square-wave voltage input $V_{ACT,p-p} = 1$ V with a frequency of 1.3 kHz, shown as a black line in Figure 3a and 3b (black curves). Figure 3a shows a measurement of the displacement of pump 1, when applying $V_{ACT}$ on pump 1 while keeping pump 2 grounded (dark blue curve) or when actuating pump 2 while keeping pump 1 grounded (light blue curve). Both curves show a main frequency component that is coinciding with the frequency of the driving signal, meaning that the detected motion is a consequence of the applied actuation.

When switching the electrostatic actuation to pump 2 it is seen that the photodiode voltage from pump 1 ($V_{PD,21}$) is 180 degrees out of phase with respect to the situation where pump 1 is electrostatically driven ($V_{PD,11}$). This shows that pump 1 moves in the opposite direction if it is indirectly driven via pump 2, compared to if it is electrostatically actuated. This observation provides evidence which shows that the indirect actuation of drum 1 (in the 21 configuration) is pneumatic, i.e. mediated by displacement of gas from one chamber to the other. The same experiments are repeated in Figure 3b when moving the laser spot to pump 2. The red curve represents the case when pump 2 is electrically actuated while keeping pump 1 grounded and the pink curve represents the case when pump 1 is being electrically actuated while keeping pump 2 grounded. The same conclusion can be drawn: the two curves are 180 degrees out-of-phase, confirming that the drums move in opposite directions.

It is noted that the photodiode signal amplitudes in Figure 3 are quite different. These differences are attributed to gap differences between the pumps that affect the actuation and detection efficiency. To prove that the indirect actuation is really gas mediated, the experiment is repeated at low pressure (Fig. 4), in which case $V_{PD,12}$ (and the motion of pump 2) is not responding to the actuation of pump 1, showing that pneumatic actuation is not detected in vacuum, as expected.

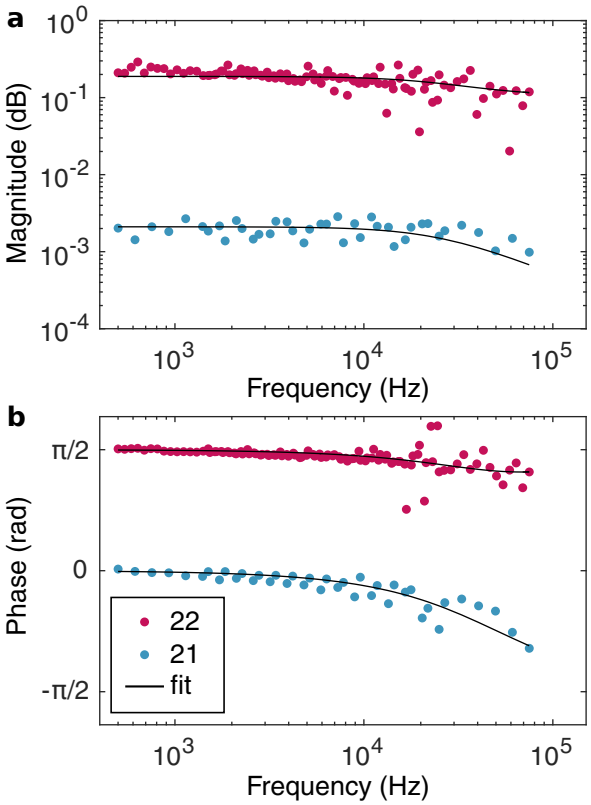


*Figure 5: Bode plots of magnitude (a) and phase (b) of the system for actuation of pump 2. The data points are colored according to the measurement scheme: the red points represent actuation and detection at pump 2, while the light blue represent actuation at pump 2 and measurement of pump 1. The fits correspond to a first order low-pass filter with cut-off frequency 25.4±2.2 kHz.*

## FREQUENCY RESPONSE

To investigate the nanoscale gas dynamics through the microchannel, the high-frequency response of the pumps is measured. The frequency of the square-wave input signal ($V_{ACT}(t)$ like in Fig. 3) is varied from 510 Hz to 23 kHz. For each actuation frequency, the Fourier transform is taken of both the input and output signal. By taking the ratio of the input and output response at each of the base driving frequencies and also at the first three higher harmonics (to increase frequency resolution), a frequency response plot is obtained and is shown as a Bode plot in Figure 5. It can be seen that both the magnitude and phase of the resulting frequency response curves are flat up to a frequency of 10 kHz. At higher frequencies the magnitude of the motion of the second drum drops, which suggests that at these frequencies the pumping efficiency starts to become limited by gas dynamics through the narrow channel. Fits show that the response of the pumps corresponds to a first-order RC low-pass filter with a cut-off frequency of 25.4±2.2 kHz.

## DISCUSSION AND CONCLUSIONS

The demonstrated graphene-based pump system is not only of extraordinarily small size (total volume of 7 femtoliter), but it is also capable of pumping very small amounts of gas: 76 attoliter of gas is pumped through the channel per cycle. The thermal noise, due to charge fluctuations on the capacitor plates, sets a lower limit to the pump rate of less than 1 zeptoliter/√Hz, which is equivalent to less than 30 molecules/√Hz at ambient pressure and room temperature. The maximum electrostatic pressure that can be generated by the graphene pump is 0.5 bar, as calculated from the measured value of the breakdown voltage of 16 V. The typical force exerted at $V_{ACT}$ =1 V is 4 nN, corresponding to a pressure of 2 mbar.

Besides the pneumatic actuation and pumping, the system also allows the study of gas dynamics in channels of sub-micron dimensions, where the free path length of molecules is longer than the channel height, even at atmospheric pressure. The presented graphene pump system can therefore be used as a platform for studying anomalous viscous effects in narrow constrictions and graphene-gas interactions at the nanoscale. It thus provides a route towards scaling down nanofluidic systems by using graphene membranes.

## ACKNOWLEDGEMENTS

This work was supported by the Netherlands Organisation for Scientific Research (NWO/OCW), as part of the Frontiers of Nanoscience (NanoFront) program and the European Union Seventh Framework Programme under grant agreement no. 604391 Graphene Flagship.

## REFERENCES

[1] W. Judy, T. Tamagawa, and D. L. Polla, Proc. IEEE MEMS, 182 (1991).
[2] R. Zengerle, A. Richter, and H. Sandmaier, Proc. IEEE MEMS, 19 (1992).
[3] D. J. Laser and J. G. Santiago, Journal of Micromechanics and Microengineering **14**, R35 (2004).
[4] B. D. Iverson and S. V. Garimella, Microfluidics and Nanofluidics **5**, 145 (2008).
[5] S. Lee, R. An, and A. J. Hunt, Nature Nanotechnology **5**, 412 (2010).
[6] J. S. Bunch, A. M. Van Der Zande, S. S. Verbridge, I. W. Frank, D. M. Tanenbaum, J. M. Parpia, H. G. Craighead, and P. L. McEuen, Science **315**, 490 (2007).
[7] A. Smith, S. Vaziri, F. Niklaus, A. Fischer, M. Sterner, A. Delin, M. Östling, and M. Lemme, Solid-State Electronics **88**, 89 (2013).
[8] R. J. Dolleman, D. Davidovikj, S. J. Cartamil-Bueno, H. S. J. van der Zant, and P. G. Steeneken, Nano Letters **16**, 568 (2016).
[9] S. P. Koenig, L. Wang, J. Pellegrino, and J. S. Bunch, Nature Nanotechnology **7**, 728 (2012).
[10] R. J. Dolleman, S. J. Cartamil-Bueno, H. S. J. van der Zant, and P. G. Steeneken, 2D Materials **4**, 011002 (2016).
[11] A. Sakhaee-Pour, M. Ahmadian, and A. Vafai, Solid State Communications **145**, 168 (2008).
[12] J. Atalaya, J. M. Kinaret, and A. Isacsson, EPL (Euro-physics Letters) **91**, 48001 (2010).
[13] D. Todorović, A. Matković, M. Milićević, D. Jovanović, R. Gajić, I. Salom, and M. Spasenović, 2D Materials **2**, 045013 (2015).
[14] Q. Zhou, J. Zheng, S. Onishi, M. Crommie, and A. K. Zettl, Proceedings of the National Academy of Sciences **112**, 8942 (2015).
[15] Q. Zhou and A. Zettl, Applied Physics Letters **102**, 223109 (2013), http://dx.doi.org/10.1063/1.4806974.
[16] J. S. Bunch, S. S. Verbridge, J. S. Alden, A. M. van der Zande, J. M. Parpia, H. G. Craighead, and P. L. McEuen, Nano Letters **8**, 2458 (2008).
[17] D. Davidovikj, P. H. Scheepers, H. S. J. van der Zant, and P. G. Steeneken, arXiv:1708.05952 (2017).
[18] A. Castellanos-Gomez, M. Buscema, R. Molenaar, V. Singh, L. Janssen, H. S. J. van der Zant, and G. A. Steele, 2D Materials **1**, 011002 (2014).

## CONTACT

P.G. Steeneken, p.g.steeneken@tudelft.nl